Interface-state-phonon-assisted energy relaxation of hot electrons in CdSe quantum dots

Shengkun Zhang[a)]
Science Department, Borough of Manhattan Community College, City University of New York, 199 Chambers Street, New York 10007

Iosif Zeylikovich
Physics and Technology Department, Bronx Community College, City University of New York, 2155 University Avenue, Bronx, New York 10453

Taposh K. Gayen, Bidyut Das, and Robert R. Alfano
Institute for Ultrafast Spectroscopy and Laser, Department of Physics, City College of New York, City University of New York, 160 Convent Avenue, New York 10031

Aidong Shen
Department of Electrical Engineering, City College of New York, City University of New York, 160 Convent Avenue, New York 10031

Maria C. Tamargo
Department of Chemistry, City College of New York, City University of New York, 160 Convent Avenue, New York 10031

(Received 13 November 2015; accepted 21 January 2016; published 11 February 2016)

The authors report experimental observation of a new electron relaxation mechanism in CdSe quantum dots (QDs), through which electrons release their excess energy by emitting interface-state phonons (ISPs). Photogenerated electrons in surrounding barrier materials are initially captured by interfacial defects and then are released into QDs. Due to the strong coupling to the interface states, these hot electrons in QDs step down to their ground state by emitting interface-state phonons. This phenomenon became observable in the microscopic photoluminescence spectra of the CdSe QDs under intense excitation of a femtosecond laser. Up to six ISP phonon replicas were observed as sub-peaks in the high-energy side of the photoluminescence peak of the quantum dots. The energy of these ISP phonons is determined to be 17 meV. The temperature dependence of this relaxation mechanism is discussed. The ISP phonons have been observed in Raman scattering spectra, and their interface feature have been identified. The experiments have proved the prediction of Sercel in Phys. Rev. B **51**, 14532 (1995), where defect levels nearby QDs were proposed to assist energy relaxation of electrons in quantum dots. However, instead of energy relaxation during the capture process from the barriers to the interfacial defects, electrons are found here to release their excess energy during the capture process from the interfacial defects to the ground state of the CdSe QDs. © *2016 American Vacuum Society*. [http://dx.doi.org/10.1116/1.4941138]

I. INTRODUCTION

Semiconductor quantum dots (QDs) become one of the major ongoing research interests in recent years. Due to their discrete energy states and tunable energy separation, quantum dots are prominent for superior performance of optoelectronic devices like QD lasers[1–4] and infrared photodetectors,[5–7] and photonic[8–10] and spintronic[11–14] devices for quantum information processing.[15] Although extensive research has been performed on quantum dots in the past decades, further understanding of QDs' fundamental physical properties is still being pursued, which is of utmost importance for all these device applications.

One mystery in semiconductor quantum dots is mechanisms of carrier energy relaxation. In an ideal quantum dot system, energy relaxation through single longitudinal-optical (LO) phonon emission is forbidden except in the unlikely case that energy level separation equals $\hbar\omega_{LO}$, which is so-called "phonon bottleneck."[16–18] In this circumstance, much longer relaxation and dephasing times could be expected, but not desired by most of the device applications. Carriers in QDs can also release their energy through Auger mechanism, whereby the excess electron energy is rapidly transferred to holes, which then relaxes rapidly through its dense spectrum of states.[19,20] Other possible mechanisms that have been theoretically proposed include electron-hole scattering,[21] multiphonon-assisted tunneling through deep levels,[22] acoustic-optical phonon interactions,[23,24] and carrier-longitudinal acoustic phonon interactions.[25]

In this paper, we report experimental observation of a new mechanism of electron relaxation in semiconductor quantum dots, through which electrons release their energy by emitting interface-state phonons (ISPs). Under intense femtosecond laser excitation at 400 nm, microscopic photoluminescence (micro-PL) experiments were performed on CdSe quantum dots surrounded by ZnCdMgSe barrier materials. Photoexcited electrons in the ZnCdMgSe barriers were found to be captured by the interface states and then be

a)Electronic mail: szhang@bmcc.cuny.edu

released into the CdSe QDs. The hot electrons relax to the ground state of the QDs through emitting interface-state phonons with phonon energy of 17 meV. The theoretical prediction of Sercel on this defect-assisted relaxation process in 1995 has been experimentally proved in this work.[22]

II. EXPERIMENT

Two CdSe/ZnCdMgSe QD samples were grown on semi-insulating InP substrates in a dual-chamber MBE system. This MBE system was designed for II-Se material growth and was described elsewhere.[26] After the removal of oxide layer under As flux and the growth of a 0.15 μm InGaAs buffer layer in the III–V growth chamber, the wafers were transferred through vacuum modules to the II–VI growth chamber. After deposition of 7 nm $Zn_{0.5}Cd_{0.5}Se$ buffer layer at 200 °C, the wafer temperature was raised to 573 K (300 °C) to grow 300 nm ZnCdMgSe buffer layer for each sample. For sample A, 2.5 monolayer of CdSe was deposited on the buffer layer followed by a 5.2 nm $Zn_{0.2}Cd_{0.2}Mg_{0.6}Se$ barrier layer. The $CdSe/Zn_{0.2}Cd_{0.2}Mg_{0.6}Se$ layers were repeatedly grown for ten times. For sample B, 3.6 monolayer of CdSe was deposited on the buffer layer followed by a 14 nm $Zn_{0.2}Cd_{0.2}Mg_{0.6}Se$ barrier layer. The $CdSe/Zn_{0.2}Cd_{0.2}Mg_{0.6}Se$ layers were repeatedly grown for 3 times. Finally, each sample was capped with a thin $Zn_{0.5}Cd_{0.5}Se$ layer. The CdSe quantum dots were self-assembled, and the actual dot sizes are unknown. Inferred from the atomic force microscopy measurement results on uncapped QDs, the height of the dots is in the range between 2.5 and 5.5 nm while the lateral size is in between 20 and 40 nm. The areal density of the QDs is about $8 \times 10^8\,cm^{-2}$. Under a 325 nm He-Cd laser excitation, the photoluminescence peaks of the CdSe QDs in samples A and B were observed at 2.438 and 2.122 eV, respectively, indicating smaller-sized QDs in sample A and larger-sized QDs in sample B. The bandgap of the $Zn_{0.2}Cd_{0.2}Mg_{0.6}Se$ barriers was determined to be 3.020 eV at room temperature by PL experiments on a separately grown $Zn_{0.2}Cd_{0.2}Mg_{0.6}Se$ sample with a thickness of 300 nm.

Microscopic photoluminescence experiments were performed using a near-field optical microscopy setup. The second harmonic radiation at 3.100 and 2.952 eV obtained from a mode-locked tunable Ti-Sapphire laser was used as PL excitation source. The laser pulses have a pulse width of 150 fs and a repetition rate of 78 MHz. The power of the second harmonic radiation can be adjusted from 0 to 18 mW by controlling the power of the Ti-Sapphire laser. After going through necessary optics, only 25% power can be left to excite samples. The second harmonic laser was focused onto the samples by an objective, and the laser spot diameter is about 5 μm. Laser power of 1 mW in a 5 μm diameter spot corresponds to a power density of $5.11\,kWcm^{-2}$, and a peak power of $0.43\,GWcm^{-2}$ for the 150 fs laser pulse in the repetition rate of 78 MHz. In a spot with a 5 μm diameter, the number of CdSe QDs is estimated to be 160 considering the QD areal density of $8 \times 10^8\,cm^{-2}$. The luminescence spectra were collected by the same objective and recorded with a cooled CCD camera integrated to a spectrometer with a resolution of 0.2 nm. The exposure time of the laser to the samples is kept as same as the integration time of the CCD camera. Raman experiments were done under 633 nm CW laser excitation with a 45° incident angle. All micro-PL and Raman experiments were carried out at room temperature.

III. RESULTS AND DISCUSSION

A. Sample A

Figure 1 shows the micro-PL spectra of sample A measured under the different excitation powers and exposure times with the femtosecond laser at 3.100 eV. The broad luminescence peak originates from radiative recombination of electrons in the ground state (S state) of the QDs. Though not specified in the spectra, luminescence from individual dots can be observed as sharp peaks with widths of about 1 meV that is limited by the spectrometer resolution of 0.2 nm. When the laser power is increased from 0.3 to 4.5 mW with 1 s exposure time, the only notable change in the PL spectra is that the PL peak shifted from 2.438 to 2.431 eV.

When increasing the exposure time to 2, 3, and 4 s while fixing the laser power at 4.5 mW, remarkable changes are observed in the PL spectra. Beside the large red shift of the PL peak, the most striking phenomenon is the appearance of subpeaks in the higher energy side of the broad PL peak. These subpeaks are equally separated in energy. The broadening of the weakest subpeak at highest energy is due to the enhanced luminescence of the first excited state (P state) of the QDs. Up to six subpeaks have been clearly seen in the PL spectrum measured with 4.5 mW laser power for 4 s.

The redshift of the main PL peak indicates temperature increase due to heating of high power laser. By measuring CW PL spectra excited by a 325 nm He-Cd laser from 77 K to room temperature, temperature dependence of emission energy of the main PL peak is linearly fitted and the temperature coefficient for sample A is determined to be −0.34 meV/K. This is close to previously reported value −0.36 meV/K.[27] The lattice temperature values for micro-PL measurements are then

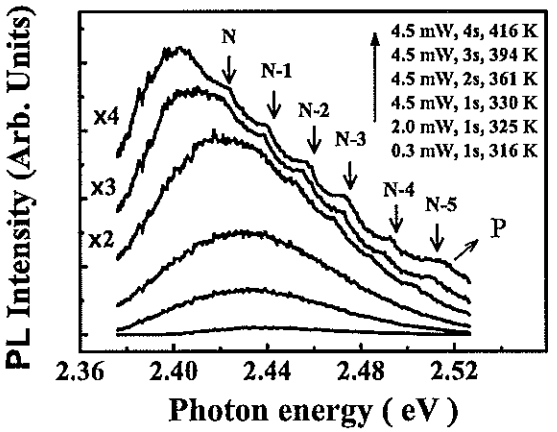

FIG. 1. Microscopic photoluminescence spectra of sample A with smaller-sized CdSe quantum dots measured under intense laser excitation with different power and exposure time. Phonon replicas are marked as N, N-1, N-2,..., N-5. The first excited state is labeled as P. Laser power, exposure time, and lattice temperature values are also listed.

TABLE I. List of energy positions of photoluminescence peaks of samples A and B, and energy separation between these PL peaks.

	Power (mW)/ time (s)	E_S (eV)	E_N (eV)	E_{N-1} (eV)	E_{N-2} (eV)	E_{N-3} (eV)	E_{N-4} (eV)	E_{N-5} (eV)	E_P (eV)	ΔE_{SP} (meV)	ΔE_{SN} (meV)	$\Delta E_{N,N-1}$ (meV)
A	4.5/4	2.403	2.423	2.440	2.457	2.474	2.491	2.508	2.514	111	20	17
	4.5/3	2.410	2.421	2.438	2.455	2.472	2.489	2.506			11	17
	4.5./2	2.424	2.434	2.451	2.468	2.485	2.502				10	17
B	2.25/1	2.095	2.110	2.127	2.144				2.153	58	15	17
	1.5/1	2.103	2.113	2.130	2.147				2.151		10	17
	1.25/1	2.106	2.114	2.131	2.148				2.151		8	17

deduced according to the linear relationship between PL energy and temperature, and are labeled in Fig. 1.

While labeling the subpeaks with N, N-1,..., N-5 in Fig. 1, the energy positions of all the subpeaks, the main peak from the S state and the peak from the P state are listed in Table I. The energy separation between these subpeaks is determined to be 17 meV, and the energy separation between the S state and the P state of the CdSe QDs is 111 meV.

B. Sample B

The same features are observed in the micro-PL spectra recorded for sample B that has larger-sized QDs. Figure 2 displays the micro-PL spectra of sample B measured at different laser powers from 0.37 to 2.25 mW with a fixed exposure time of 1 s. Beside those measured under 3.100 eV laser excitation (solid lines), Fig. 2 also shows the PL spectrum measured under 2.952 eV laser excitation with the power of 2 mW (dotted line). Three subpeaks are clearly observed in the higher energy side of the main PL peak in the spectrum recorded at 2.25 mW. This subpeak feature starts to appear at 0.5 mW for sample B. Same as the observation in sample A, the luminescence peak of the P state appears in the high energy tail with high power excitation. Note that when the photon energy of laser is tuned to 2.952 eV, which is below the bandgap of the ZnCdMgSe barriers, no subpeak feature has been observed though the laser power is as high as

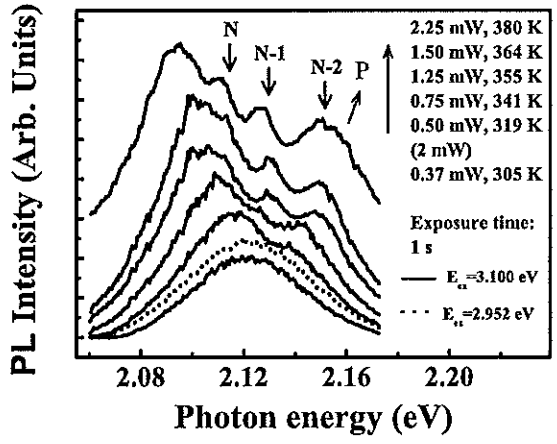

FIG. 2. Microscopic photoluminescence spectra of the CdSe QD sample B with larger-sized CdSe quantum dots measured under intense laser excitation with different power and a fixed exposure time of 1 s. Three phonon replicas are marked as N, N-1, and N-2. The first excited state is labeled as P. Laser power and lattice temperature values are also listed.

2 mW, and the PL intensity is even lower than that measured at 0.5 mW with the 3.100 eV laser.

By measuring CW PL spectra from 77 K to room temperature, temperature dependence of emission energy of the main PL peak is linearly fitted, and the temperature coefficient for sample B is determined to be −0.30 meV/K. The lattice temperature values for micro-PL measurements are then deduced according to the PL redshift and labeled in Fig. 2.

While labeling the subpeaks with N, N-1, and N-2 in Fig. 2, the energy positions of the subpeaks and the PL peaks from the S state and the P state are listed in Table I. The energy separation between these subpeaks is determined to be 17 meV, and the energy separation between the S state and the P state of the CdSe QDs is 58 meV. The lower PL energy of the S state and the smaller energy separation between the S and P states in sample B is consistent with the weaker quantum confinement in its larger-sized QDs.

C. Discussion

The red shift of the PL peak of the S state results from heating effect of the intense laser excitation. For sample A, the lattice temperature is found to increase from 316 K with 0.3 mW and 1 s excitation to 416 K with 4.5 mW and 4 s excitation. For sample B, the lattice temperature increased from 305 K with 0.37 mW and 1 s excitation to 380 K with 2.25 mW and 1 s excitation. For the fixed excitation power of 4.5 mW, the integration time of the CCD camera was kept the same while the laser exposure time was increased from 1 to 2, 3, and 4 s, respectively. If averaging the PL intensity by time, the PL intensity in a fixed integration time decreases with the increasing of exposure time for the fixed power of 4.5 mW, which is due to thermal quenching of PL during exposure time.

The most remarkable feature in the PL spectra of samples A and B is the appearance of subpeaks in the higher energy side of the PL peaks of the S states. In the following, we will demonstrate that this new feature cannot be explained by any currently known mechanisms. Obviously, the equal energy separation 17 meV of these subpeaks indicates phonon involvement during the electron relaxation process. The most common explanation for such a feature is that hot electrons emit LO phonons of CdSe QDs. But the LO phonon energy of CdSe is 26.5 meV,[28,29] which is about 50% larger than the energy separation of 17 meV. Either strain or quantum confinement cannot account for such large reduction of LO phonon energy.[30] In fact, our previous Raman

experiments on self-assembled CdSe QDs have shown that the LO phonon energy of self-assembled CdSe QDs is about 27 meV corresponding to a wavenumber of 220 cm^{-1}.[31]

Another possible origin of these phonons with 17 meV energy is interface phonons localized at the CdSe QD/ZnCdMgSe interface. The mode frequencies of interface phonons of quantum dots depend strongly on the dot size and shape[32,33] and are intermediate between those of TO and LO modes of the interface materials.[32,34] We have two reasons to conclude that the phonon replica features observed in this work are not from interface phonons. First, for the phonon energy of 17 meV, the corresponding mode frequency of the observed phonons is 137 cm^{-1}, which is not intermediate between those of TO and LO phonons of CdSe and ZnCdMgSe materials, and is much lower than the lowest frequency of those phonons. For instance, the lowest phonon frequency of CdSe and ZnCdMgSe materials is 169 cm^{-1},[28,29,35] the frequency of TO phonons in CdSe, which is 32 cm^{-1} larger than that of the observed phonons. Second, the frequency of the observed phonons does not depend on the dot size. It is the same in the either smaller-sized (sample A) or larger-sized (sample B) CdSe QDs.

We propose that the observed phonon replica features are from interface states at the CdSe QD/ZnCdMgSe interface. These interface states are interfacial defects induced by lattice mismatch or interface roughness. Our recent study of time-resolved PL has confirmed the existence of the interface states in ZnCdSe/ZnCdMgSe quantum wells.[36] The density of these interface states was found to increase with decreasing quantum well thickness. These interface defects could not be induced by heating effect of laser pulse excitation because the highest lattice temperature 416 K is much lower than material growth temperature 573 K (300 °C).

In order to identify the vibration modes of these interface states, Raman scattering experiments were performed on samples A, B, and a control sample under 633 nm CW laser excitation with a 45° incident angle. The results are shown in Fig. 3. The control sample has the same structure parameters and growth procedure except having only one layer of CdSe QDs. The dashed-lined arrows indicate the scattering lines of CdSe QDs, ZnCdSe, ZnCdMgSe, and InGaAs, respectively. For each sample, a strong and broad scattering peak has been observed in the wavenumber range from 80 to 220 cm^{-1}. And it peaks at 137 cm^{-1}, which corresponds to 17 meV and equals to the phonon energy derived from the PL spectra. This indicates the same origin of the broad Raman peak and the PL subpeaks in Figs. 1 and 2. For the control sample with a single layer of CdSe QDs, the scattering peak of LO phonons in CdSe QDs is seen at 220 cm^{-1}. As for samples A and B, the scattering intensity of the broad peak is so strong that it covers the scattering peak of CdSe QDs' LO phonons.

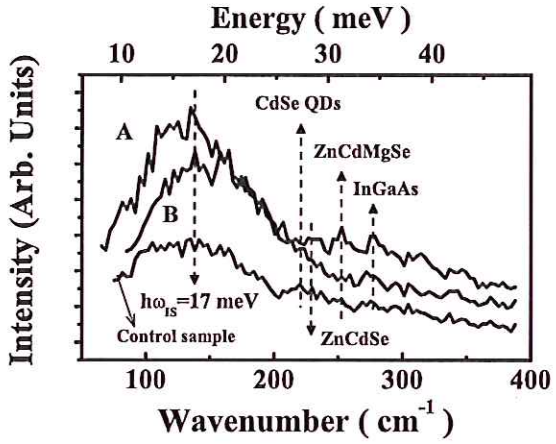

FIG. 3. Raman scattering spectra of samples A and B, and a control sample with a single layer of CdSe QDs.

The scattering peak is broad in the range of 80–220 cm^{-1}, and its intensity depends on the number of QD layers. This indicates that it originates from interface states. The Raman scattering from many different interface states leads to this broad peak. And with the increasing of the number of QD layers as well as the number of CdSe QD/ZnCdMgSe interfaces, e.g., 1 QD layer in the control sample, 3 QD layers in sample B, and 10 QD layers in sample A, the scattering intensity increases accordingly. These interface states may induce many vibration modes, and produce ISPs with different frequencies. It is not clear that whether all these interface-state phonons involve in the electron relaxation process. It is possible that only interface-state phonons with particular frequencies are responsible for the phonon replica feature of the PL spectra of samples A and B. If so, the phonons with sharp Raman peaks located at 17 meV for sample B and at 16.8 meV for sample A will most likely be the active ones. We can conclude that the hot electrons in the CdSe QDs of samples A and B relax through emitting interface-state phonons and the phonon energy of the most active phonons is about 17 meV.

We further testify that the hot electrons that emit interface-state phonons come from the photogenerated electrons in the barrier materials. These electrons couple with the interface-state phonons while crossing the interface. The direct evidence supporting this conclusion is that the phonon replica features can only be observed while the photon energy of the laser is higher than the bandgap of the ZnCdMgSe barriers. As shown in Fig. 2, the phonon effect becomes visible for sample B at the laser power as low as 0.5 mW when the photon energy of the laser is 3.100 eV, 80 meV larger than the bandgap of the barriers. When the photon energy of the laser is tuned to 2.952 eV that is about 70 meV below the bandgap of the barriers, no phonon replica could be seen even at the laser power as high as 2 mW. This is because that much less carrier could transfer from barrier to QDs under excitation below bandgap of barrier. The PL intensity of the ground state of the CdSe QDs is much lower with 2.952 eV excitation than that with 3.100 eV excitation because of the less carrier population in the QDs.

A schematic energy band diagram of CdSe QD/ZnCdMgSe structure is presented in Fig. 4 to illustrate the electron relaxation process assisted by interface-state phonons. Under laser excitation, electrons are generated in the ZnCdMgSe barrier material and then captured by the CdSe QD. While crossing the QD/barrier interface, the electrons

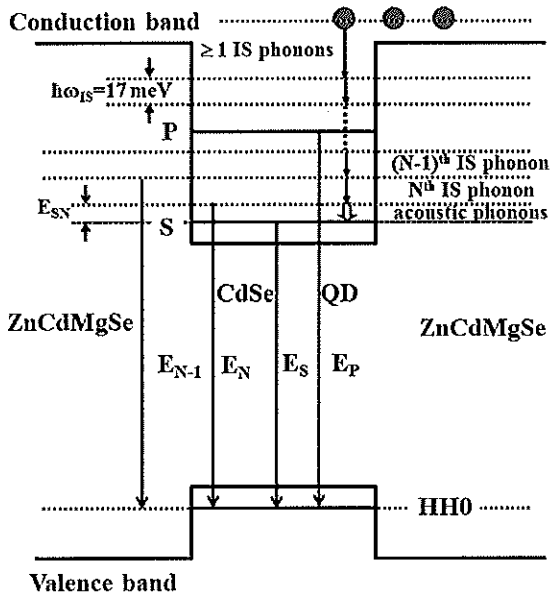

FIG. 4. Schematic energy band diagram to show electron relaxation process assisted by interface-state phonons in CdSe/ZnCdMgSe quantum dots.

couple with interface-state phonons and start to relax in the QD by emitting these phonons. The phonon energy of the most active interface-state phonons is about 17 meV. It is unclear whether the electrons will emit multiple phonons at one time in the initial step of the relaxation process. However, it is clear that they release interface-state phonons one by one when approaching the electron ground state of the QD. At the same time, part of these electrons emit photons through radiative recombination with the holes on the hole ground state in the valence band. The simultaneous emission of photons and phonons produces the subpeaks of the PL spectra in Figs. 1 and 2. After emitting multiple interface-state phonons, the electrons approach their ground state in an energy difference less than one phonon energy. They will release their rest energy and relax to their ground state by emitting acoustic phonons. The values of ΔE_{SN} listed in Table I, which is the energy difference between E_S and E_N, are all comparable or less than 17 meV, thus supporting our Conclusion.

The maximum value of N can be estimated by dividing the maximum excess energy of electrons by one ISP phonon energy. Providing a ratio of conduction band offset of 80%, the energy difference between the electron ground state of the QD and the bottom of conduction band of the barrier is calculated to be about 550 meV for sample A, and about 800 meV for sample B. Accounting the 80 meV kinetic energy provided by laser photons, the total excess energy of electrons is 630 meV for sample A and 880 meV for sample B. Dividing the total excess energy by 17 meV, the maximum integer of N is calculated to be 37 for sample A and 51 for sample B.

The experimental data support Sercel's theory of defect-level-assisted electron relaxation.[22] In this theory, a free electron in barrier materials is captured into the ground state of a quantum dot mediated by a defect level, which is most likely to be interface states. The electron is captured by the defect level and relaxes to the ground state of the defect level through multiphonon emission process.[37] In the configuration coordinate diagram, when the energy of the electron at the defect level vibrates and reaches up to a crossing point between the defect level and the ground state of the QD, the electron can transit into the QD. In high temperature limit, the expression of the transition rate takes the thermally activated form and is proportional to $\exp(-Ea/kT)$, where Ea is the activation energy. This means that the transition rate will be greatly increased with the increasing of temperature. Our experimental data agree very well with this prediction. It can be seen from Figs. 1 and 2 that phonon replica appears and increases its number with increasing of temperature. Sercel's theory is further supported by the appearing of the PL peaks of the excited states at higher temperatures, as shown in Figs. 1 and 2. Similar to that for electron transition to the ground state, the expression of the transition rate accounting for transition to the first excited state is proportional to $\exp(-Ea'/kT)$, where Ea′ is the activation energy for the first excited state. The first excited state has higher activation energy and requires higher temperature to initiate relaxation assisted by interface state phonons. This is experimentally observed as arising of the high energy band when temperature is increased. This could not be explained by direct band-to-band transition because PL should be quenched but not be enhanced at higher temperature in that case.

Hot electrons generated in barriers relax to ground state of quantum dots by two separate processes. First, as illustrated by Sercel's theory, electrons in barriers release energy through multiphonon emission and then captured by defect level. Second, electrons are thermally activated from defect level to QD ground state and continue to release excess energy by emitting interface state phonons. If interface defects form strong vibration modes at the interface, electrons prefer releasing their excess energy by emitting interface-state phonons instead of lattice phonons. The second process is not considered in Sercel's theory.

IV. CONCLUSIONS

This work reports experimental observation of a new electron relaxation mechanism in CdSe/ZnCdMgSe quantum dots. Upon strong coupling with interface states, electrons are found to cool down to their ground state through emitting interface-state phonons with the phonon energy of 17 meV. These interface-state phonons have been identified by Raman scattering measurements. Our experiments strongly support Sercel's theory on defect-assisted electron relaxation that is thermally activated. The intense and near resonant laser excitation to the barrier materials provided sufficient source electrons in the barriers and ensured the successful observation of this mechanism in our micro-PL experiments. We believe that interface-state-phonon assisted electron relaxation is a general mechanism existing in semiconductor interfaces. This finding will benefit the development of QD-based optoelectronic and photonic devices.

ACKNOWLEDGMENT

The authors thank the support of Professional Staff Congress of the City University of New York with Grant Award PSC-CUNY No. 68478-00 46.

[1]Z. R. Lv, H. M. Ji, S. Luo, F. Gao, F. Xu, D. H. Xiao, and T. Yang, AIP Adv. **5**, 107115 (2015).
[2]Y. C. Wu, L. Jiang, and L. V. Asryan, J. Appl. Phys. **118**, 183107 (2015).
[3]V. I. Klimov, A. A. Mikhailovsky, S. Xu, A. Malko, J. A. Hollingsworth, C. A. Leatherdale, H.-J. Eisler, and M. G. Bawendi, Science **290**, 314 (2000).
[4]S. M. Kim, Proc. SPIE **4999**, 423 (2003).
[5]X. J. Wang, S. Q. Zhai, N. Zhuo, J. Q. Liu, F. Q. Liu, S. M. Liu, and Z. G. Wang, Appl. Phys. Lett. **104**, 171108 (2014).
[6]H. Lim, W. Zhang, S. Tsao, T. Sills, J. Szafraniec, K. Mi, B. Movaghar, and M. Razeghi, Phys. Rev. B **72**, 085332 (2005).
[7]G. Konstantatos, I. Howard, A. Fischer, S. Hoogland, J. Clifford, E. Klem, L. Levina, and E. H. Sargent, Nature **442**, 180 (2006).
[8]T. Reichert *et al.*, Phys. Rev. B **90**, 115310 (2014).
[9]A. Zrenner, E. Beham, S. Stufler, F. Findeis, M. Bichler, and G. Abstreiter, Nature **418**, 612 (2002).
[10]A. Kolli, B. W. Lovett, S. C. Benjamin, and T. M. Stace, Phys. Rev. Lett. **97**, 250504 (2006).
[11]A. Ghosh and H. O. Frota, J. Appl. Phys. **114**, 073707 (2013).
[12]J. D. Mar, X. L. Xu, J. J. Baumberg, F. S. F. Brossard, A. C. Irvine, C. Stanley, and D. A. Williams, Phys. Rev. B **83**, 075306 (2011).
[13]F. H. L. Koppens, C. Buizert, K. J. Tielrooij, I. T. Vink, K. C. Nowack, T. Meunier, L. P. Kouwenhoven, and L. M. K. Vandersypen, Nature **442**, 766 (2006).
[14]R. Hanson and G. Burkard, Phys. Rev. Lett. **98**, 050502 (2007).
[15]A. Olaya Castro and N. F. Johnson, "Quantum information processing in nanostructures," in *Handbook of Theoretical and Computational Nanothechnology*, edited by M. Rieth and W. Schommers (American Scientific, Valencia, CA, 2005), Vol. 7.
[16]U. Bockelmann and G. Bastard, Phys. Rev. B **42**, 8947 (1990).
[17]H. Benisty, C. M. Sotomayor Torres, and C. Weisbuch, Phys. Rev. B **44**, 10945 (1991).
[18]J. Urayama, T. B. Norris, J. Singh, and P. Bhattacharya, Phys. Rev. Lett. **86**, 4930 (2001).
[19]A. L. Efros, V. A. Kharchenko, and M. Rosen, Solid State Commun. **93**, 281 (1995).
[20]V. I. Klimov, J. Phys. Chem. B **104**, 6112 (2000).
[21]I. Vurgaftman and J. Singh, Appl. Phys. Lett. **64**, 232 (1994).
[22]P. C. Sercel, Phys. Rev. B **51**, 14532 (1995).
[23]T. Inoshita and H. Sakaki, Phys. Rev. B **46**, 7260 (1992).
[24]T. Inoshita and H. Sakaki, Phys. Rev. B **56**, R4355 (1997).
[25]A. Bertoni, M. Rontani, G. Goldoni, and E. Molinari, Phys. Rev. Lett. **95**, 066806 (2005).
[26]L. Zeng, S. P. Guo, Y. Y. Luo, W. Lin, M. C. Tamargo, H. Xing, and G. S. Cargill III, J. Vac. Sci. Technol., B **17**, 1255 (1999).
[27]T. J. Liptay and R. J. Ram, Appl. Phys. Lett. **89**, 223132 (2006).
[28]D. V. Melnikov and W. Beall Fowler, Phys. Rev. B **64**, 245320 (2001).
[29]*Semiconductors: Basic Data*, edited by O. Madelung (Springer, Berlin, 1996).
[30]R. W. Meulenberg, T. Jennings, and G. F. Strouse, Phys. Rev. B **70**, 235311 (2004).
[31]J. S. Reparaz, A. R. Goñi, M. I. Alonso, M. N. Perez-Paz, and M. C. Tamargo, Appl. Phys. Lett. **89**, 231109 (2006).
[32]P. A. Knipp and T. L. Reinecke, Phys. Rev. B **46**, 10310 (1992).
[33]Yu. A. Pusep, G. Zanelatto, S. W. da Silva, J. C. Galzerani, P. P. Gonzalez-Borrero, A. I. Toropov, and P. Basmaji, Phys. Rev. B **58**, R1770 (1998).
[34]R. Englman and R. Ruppin, Phys. Rev. Lett. **16**, 898 (1966).
[35]A. K. Arora and A. K. Ramdas, Phys. Rev. B **35**, 4345 (1987).
[36]S. K. Zhang, H. Lu, W. B. Wang, B. B. Das, N. Okoye, M. Tamargo, and R. R. Alfano, J. Appl. Phys. **101**, 023111 (2007).
[37]C. H. Henry and D. V. Lang, Phys. Rev. B **15**, 989 (1977).